

Analytical calculation of the amplification and angular divergence of the stimulated backscattered light from a Gaussian hot spot

Laurent Divol

Commissariat à l'Énergie Atomique, Centre d'Études de Limeil-Valenton, 94195 Villeneuve-St.-Georges Cedex, France

Philippe Mounaix

Centre de Physique Théorique, Ecole Polytechnique, 91128 Palaiseau Cedex, France

(Received 16 December 1997)

The problem of backscattering instabilities from a single laser hot spot is considered analytically in the frame of the paraxial approximation. An analytical calculation of the convective gain and of the far-field angular divergence of the backscattered light is presented for both homogeneous and inhomogeneous plasmas. It is shown that the far-field angular divergence is determined by the propagation of the backscattered light not only *within* the amplification region but also *outside* it, where the coupling is very weak. For homogeneous plasmas, the far-field angular divergence computed at the end of the interaction region is always less than what it would be if it were computed at the end of the amplification region. For inhomogeneous plasmas, both the power and the far-field angular divergence of the backscattered beam depend on the sign of the inhomogeneity gradient. [S1063-651X(98)10308-2]

PACS number(s): 52.40.Nk, 52.35.Mw, 52.35.Nx

I. INTRODUCTION

Much experimental and theoretical work has been devoted to the study of backscattering instabilities from optically smoothed laser beams. In the case of spatially smoothed beams, such as random phase plate (RPP) beams, these instabilities develop in many small scale hot spots (or speckles) randomly distributed in the interaction region. The regimes currently of practical interest correspond to situations where the macroscopic reflectivity of the plasma is determined by a few hot spots of high intensity. In these regimes, the instability is assumed to be properly described by the so-called "independent hot spot model" [1] characterized by (i) an independent description of the backscattering instability from each single intense hot spot, and (ii) averaging over the hot spot intensity to obtain the overall (macroscopic) reflectivity. Step (i) of this model can be carried out because each hot spot of sufficiently high intensity can be approximated near its maximum by a *given*, i.e., nonstochastic, intensity profile [2]. This intensity profile (e.g., that of a Gaussian beam near the focal point) depends on the geometry of the RPP elements and is the same for each hot spot.

A comprehensive theory of backscattering instabilities from a RPP field based on the independent hot spot model implies thus that one first studies backscattering instabilities from a single isolated hot spot. So far, most of such studies have been done numerically [3]. Recently, Eliseev *et al.* [4] and Tikhonchuk, Mounaix, and Pesme [5] have analytically studied the effects of diffraction on stimulated Brillouin scattering from a single hot spot. Restricting themselves to the case where the interaction length is much smaller than the hot spot itself, these authors have considered a simple model in which the spatial dependence of the speckle intensity (and, more generally, of the coupling between the daughter waves) is purely radial. In this limit, they have shown that diffraction effects can significantly lower the Brillouin reflectivity [4,5] and they have obtained expressions for the angular di-

vergence of the backscattered light in the far-field zone [5]. This paper is devoted to revisiting this problem analytically for *any* value of the interaction length and *without* neglecting the longitudinal dependence of the coupling between the daughter waves. We show that for a long enough interaction region, the coupling outside the amplification region can significantly modify the phase structure of the backscattered beam, although it is negligible for what concerns the amplification. As a result, the far-field angular divergence of the backscattered beam computed at the end of the interaction region can be significantly different from what it would be if it was computed at the end of the amplification region. We give expressions for the angular divergence of the backscattered light in the far-field zone that take this effect into account and generalize the results of Ref. [5].

In the first part of the paper, we reconsider the same problem as Eliseev *et al.* [4] in which the plasma is homogeneous and the longitudinal dependence of the coupling reduces to that of the hot spot intensity. In Sec. II we introduce our theoretical model. In Sec. III we solve the problem of the propagation of the backscattered light through the interaction region and we give the expressions of the convective gain. Section IV is devoted to the study of the the angular divergence of the backscattered beam without assuming any *a priori* ordering between the interaction and the hot spot lengths. In the second part of the paper, we reconsider the same problem as Tikhonchuk, Mounaix, and Pesme [5] in which the plasma is inhomogeneous and the longitudinal dependence of the coupling is only due to the inhomogeneity. In Sec. V we introduce our theoretical model. In Sec. VI we solve the problem of the propagation of the backscattered light through the interaction region. Section VII is devoted to the study of the convective amplification and the angular divergence of the backscattered beam. In Sec. VIII we compare our results with those of the simpler model where the longitudinal dependence of the coupling is neglected.

II. HOMOGENEOUS PLASMA: DESCRIPTION OF THE MODEL

As in Ref. [4], we will restrict ourselves to a range of parameters where neither self-focusing nor pump depletion occur. We start from the standard wave coupling equations in the linear regime, including diffraction terms in the paraxial approximation

$$\left[\partial_t + \nu_1 + V_1 \left(\partial_z - \frac{i}{2k_1} \nabla_\perp^2 \right) \right] a_1 = \gamma_0 a_2^* + S_1, \quad (1a)$$

$$\left[\partial_t + \nu_2 + V_2 \left(\partial_z + \frac{i}{2k_2} \nabla_\perp^2 \right) \right] a_2 = \gamma_0 a_1^* + S_2. \quad (1b)$$

Here a_1 and a_2 stand for the amplitude of the backscattered and electrostatic wave, respectively. The incoming laser light is assumed to propagate from right to left. The quantities V_α , ν_α , and k_α denote the group velocity, the linear damping, and the wave number of wave α , respectively (with $V_1 > 0$ and $k_\alpha > 0$). The coupling constant γ_0 is the linear homogeneous growth rate of the instability. The source terms S_α are stochastic functions in space and time that account for the thermal noise emission of each wave. In the following we will take for S_α a white noise in space and time with the statistical properties

$$\langle S_\alpha(\mathbf{x}_\perp, z, \omega) \rangle = 0,$$

$$\begin{aligned} \langle S_\alpha(\mathbf{x}_\perp, z, \omega) (S_\alpha^*(\mathbf{x}'_\perp, z', \omega')) \rangle \\ = (2\pi)^3 \Sigma_\alpha \delta^2(\mathbf{x}_\perp - \mathbf{x}'_\perp) \delta(z - z') \delta(\omega + \omega'), \end{aligned}$$

where the constant Σ_α is chosen such that one recovers the equilibrium fluctuation level of wave α when $\gamma_0 = 0$. Neglecting both the inverse bremsstrahlung absorption and the thermal noise emission of the electromagnetic waves (i.e., $\nu_1 = 0$ and $S_1 = 0$), and considering the saturated convective regime where the low frequency wave a_2 is locally enslaved to the electromagnetic wave a_1 (i.e., $V_2 = 0$), one obtains the system

$$\left[\partial_t + V_1 \left(\partial_z - \frac{i}{2k_1} \nabla_\perp^2 \right) \right] a_1 = \gamma_0 a_2^*, \quad (2a)$$

$$(\partial_t + \nu_2) a_2 = \gamma_0 a_1^* + S_2. \quad (2b)$$

Defining the Laplace transform as $a(\omega) = (2\pi)^{-1} \int_0^\infty \exp(i\omega t) a(t) dt$ and neglecting the initial condition terms, one can recast the system (2a) and (2b) into the equation

$$\left[\partial_z - \frac{i\omega}{V_1} - \frac{i}{2k_1} \nabla_\perp^2 - \frac{|\gamma_0|^2}{V_1(\nu_2 - i\omega)} \right] a_1(\omega) = \frac{\gamma_0 (S_2^*)(\omega)}{V_1(\nu_2 - i\omega)}, \quad (3)$$

with

$$|\gamma_0(\mathbf{x}_\perp, z)|^2 = \frac{\gamma^2}{1 + (z/z_R)^2} \exp\left[-\frac{x_\perp^2}{a_0^2(1 + z^2/z_R^2)} \right], \quad (4)$$

where a_0 is the hot spot waist and z_R is the Rayleigh length defined by $z_R \equiv k_1 a_0^2$. In this paper we will restrict ourselves to the physical cases characterized by the ordering $a_0 \ll z_R$. In the following Eq. (4) will be referred to as a ‘‘Gaussian’’ hot spot. Since, in the large amplification limit, one expects gain narrowing to make the backscattered beam much more localized transversally than the pump beam, one can expand the Gaussian on the left-hand side of Eq. (4) up to the first order in x_\perp^2 . Defining then \tilde{a}_1 by

$$a_1(\omega) = \tilde{a}_1(\omega) \exp(\vartheta),$$

with

$$\vartheta = \frac{i\omega(z - z')}{V_1} + \frac{\gamma^2 z_R}{V_1(\nu_2 - i\omega)} \left[\tan^{-1}\left(\frac{z}{z_R}\right) - \tan^{-1}\left(\frac{z'}{z_R}\right) \right],$$

where z' is an arbitrary point, one finds that the evolution (in z) of \tilde{a}_1 is given by a Schrödinger-like equation for a driven two-dimensional harmonic oscillator with a time-dependent complex pulsation (here the z coordinate plays the role of time). Namely, one obtains

$$\begin{aligned} \left(\partial_z - \frac{i}{2k_1} \nabla_\perp^2 + \frac{\gamma^2}{V_1(\nu_2 - i\omega)} \frac{x_\perp^2}{a_0^2 [1 + (z/z_R)^2]^2} \right) \tilde{a}_1(\omega) \\ = \frac{\gamma (S_2^*)(\omega) \exp(-\vartheta)}{V_1(\nu_2 - i\omega)(1 + iz/z_R)}. \end{aligned} \quad (5)$$

III. CONVECTIVE AMPLIFICATION BY A GAUSSIAN HOT SPOT

To solve Eq. (3) one has therefore to determine the propagator \tilde{K}_ω of the left-hand side of Eq. (5) defined as the retarded solution to

$$\begin{aligned} \left(\partial_z - \frac{i}{2k_1} \nabla_\perp^2 + \frac{\gamma^2}{V_1(\nu_2 - i\omega)} \frac{x_\perp^2}{a_0^2 [1 + (z/z_R)^2]^2} \right) \\ \times \tilde{K}_\omega(\mathbf{x}_\perp, z, \mathbf{x}'_\perp, z') = 0, \end{aligned} \quad (6)$$

with $\lim_{z \rightarrow z'} \tilde{K}_\omega(\mathbf{x}_\perp, z, \mathbf{x}'_\perp, z') = \delta^2(\mathbf{x}_\perp - \mathbf{x}'_\perp)$. Following the method of Ref. [6] it turns out that an exact closed-form solution to Eq. (6) can be obtained analytically (cf. the appendix). Transforming back to $K_\omega = \tilde{K}_\omega \exp(\vartheta)$, one finds that the full propagator of Eq. (3) is given by

$$\begin{aligned} K_\omega(\mathbf{x}_\perp, z, \mathbf{x}'_\perp, z') \\ = \frac{k_1 \alpha(\omega) \exp[i\omega z_R(\tilde{z} - \tilde{z}')/V_1 + G]}{2i\pi z_R \sqrt{1 + \tilde{z}^2} \sqrt{1 + \tilde{z}'^2} \sinh(\phi)} \\ \times \exp\left\{ \frac{ik_1}{2z_R} [\zeta x_\perp^2 + \zeta' x_\perp'^2 + 2\eta \mathbf{x}_\perp \cdot \mathbf{x}'_\perp] \right\}, \end{aligned} \quad (7)$$

where $\tilde{z} = z/z_R$, and with

$$G = G_R(\omega)[\tan^{-1}(\tilde{z}) - \tan^{-1}(\tilde{z}')],$$

$$\zeta = \frac{\alpha(\omega)\coth(\phi) + \tilde{z}}{1 + \tilde{z}^2},$$

$$\zeta' = \frac{\alpha(\omega)\coth(\phi) - \tilde{z}'}{1 + \tilde{z}'^2},$$

$$\eta = \frac{-\alpha(\omega)}{\sinh(\phi)\sqrt{1 + \tilde{z}^2}\sqrt{1 + \tilde{z}'^2}},$$

where $G_R(\omega) = \gamma^2 z_R / V_1(\nu_2 - i\omega)$ is the convective gain per

Rayleigh length for the ω component, $\alpha(\omega) = [2iG_R(\omega) - 1]^{1/2}$, and $\phi = \alpha(\omega)[\tan^{-1}(\tilde{z}) - \tan^{-1}(\tilde{z}')]$.

One can now compute the two-point correlation function at the end of the speckle centered at $z=0$ and extending from $-z_0$ to $+z_0$ [i.e., the right-hand side of Eq. (4) is multiplied by $H(z_0^2 - z^2)$ where H is the Heaviside step function]. From the solution to Eq. (3) one obtains straightforwardly

$$\langle a_1(\mathbf{x}_\perp, z_0) a_1^*(\mathbf{x}'_\perp, z_0) \rangle = \int_\omega I_\omega(\mathbf{x}_\perp, \mathbf{x}'_\perp, z_0) d\omega, \quad (8)$$

with

$$I_\omega(\mathbf{x}_\perp, \mathbf{x}'_\perp, z_0) = \frac{\gamma^2 z_R}{V_1^2(\omega^2 + \nu_2^2)} (2\pi)^3 \Sigma_2 \int_{x''_\perp} \int_{-\tilde{z}_0}^{\tilde{z}_0} \frac{K_\omega(\mathbf{x}_\perp, z_0, \mathbf{x}''_\perp, z'') K_\omega^*(\mathbf{x}'_\perp, z_0, \mathbf{x}''_\perp, z'')}{1 + \tilde{z}''^2} d^2 x''_\perp d\tilde{z}'' . \quad (9)$$

In the large gain factor limit of practical interest, the behavior of Eq. (8) is determined by the most unstable component $\omega=0$ and one has $\langle a_1(\mathbf{x}_\perp, z_0) a_1^*(\mathbf{x}'_\perp, z_0) \rangle \sim I_0(\mathbf{x}_\perp, \mathbf{x}'_\perp, z_0)$. The z integration in Eq. (9) for I_0 can then be performed using a steepest-descent method; one obtains

$$I_0(\mathbf{x}_\perp, \mathbf{x}'_\perp, z_0) \sim \frac{2\pi^2 \Sigma_2 k_1 \delta_0}{\nu_2 V_1 z_R (1 + \tilde{z}_0^2)} \exp[4G_R \tan^{-1}(\tilde{z}_0)] \times \exp\left[\frac{k_1}{2z_R(1 + \tilde{z}_0^2)} (\mu_0 x_\perp^2 + \mu_0^* x_\perp'^2 + 2\delta_0 \mathbf{x}_\perp \cdot \mathbf{x}'_\perp) \right], \quad (10)$$

with

$$\mu_0 = i[\alpha \coth(\phi_0) + \tilde{z}_0] - \frac{\alpha^2}{2 \sinh(\phi_0)^2 \text{Im}[\alpha \coth(\phi_0)]},$$

$$\delta_0 = \frac{1}{2} \left| \frac{\alpha}{\sinh(\phi_0)} \right|^2 \frac{1}{\text{Im}[\alpha \coth(\phi_0)]},$$

and where all the functions of z, z' , and ω must be evaluated at $z=z_0, z'=-z_0$, and $\omega=0$. Namely, $G_R \equiv G_R(\omega=0)$, $\alpha \equiv \alpha(\omega=0)$, and $\phi_0 = 2\alpha \tan^{-1}(z_0/z_R)$.

The validity domain of Eq. (10) reads $2G_R \tan^{-1}(z_0/z_R) \gg 1$, which follows from the large gain factor limit needed to apply the steepest-descent method in Eq. (9) (integrating first over x''_\perp and making the change of variable $u = \tan^{-1}(z_0/z_R)$, one is led to a simple exponential integration). Note that in this limit the backscattered beam is always more localized transversally than the hot spot itself, which justifies the expansion of the Gaussian in Eq. (4) *a posteriori*. The quantity $I_0(\mathbf{x}_\perp, \mathbf{x}'_\perp = \mathbf{x}_\perp, z_0)$ is proportional to the backscattered intensity at the end of the interaction region.

Integrating this quantity over x_\perp , it follows from Eq. (10) that the convective gain for the backscattered power is given by

$$G_{conv} = 4G_R \tan^{-1}\left(\frac{z_0}{z_R}\right) \quad (11)$$

in the limit $\text{Re}(\phi_0) \approx (4G_R)^{1/2} \tan^{-1}(z_0/z_R) \ll 1$, and by

$$G_{conv} = 4G_R \tan^{-1}\left(\frac{z_0}{z_R}\right) - 2 \text{Re}(\phi_0) \approx 4G_R \left(1 - \frac{1}{\sqrt{G_R}}\right) \tan^{-1}\left(\frac{z_0}{z_R}\right) \quad (12)$$

in the opposite limit $\text{Re}(\phi_0) \approx (4G_R)^{1/2} \tan^{-1}(z_0/z_R) \gg 1$. The latter equation (12), which can be rewritten as $G_{conv} = 2G_{1D}(1 - G_R^{-1/2})$, where $G_{1D} \equiv 2G_R \tan^{-1}(z_0/z_R)$ is the on-axis ($x_\perp=0$) one-dimensional gain for the amplitude, generalizes the results of Ref. [4] to an arbitrary value of the interaction length z_0 .

IV. ANGULAR DIVERGENCE OF THE BACKSCATTERED BEAM IN THE FAR-FIELD ZONE

Assuming that for $z > z_0$ the backscattered light propagates in vacuum, one has (in the paraxial approximation)

$$\begin{aligned} \langle |a_1(\mathbf{x}_\perp, z > z_0)|^2 \rangle &= \int_{x'_\perp} \int_{x''_\perp} K_{vac}(\mathbf{x}_\perp - \mathbf{x}'_\perp, z - z_0) \\ &\quad \times K_{vac}^*(\mathbf{x}_\perp - \mathbf{x}''_\perp, z - z_0) \\ &\quad \times \langle a_1(\mathbf{x}'_\perp, z_0) a_1^*(\mathbf{x}''_\perp, z_0) \rangle \\ &\quad \times d^2 x'_\perp d^2 x''_\perp, \end{aligned} \quad (13)$$

with

$$K_{vac}(\mathbf{x}_\perp, z) \equiv \frac{k_1}{2i\pi z} \exp\left(\frac{ik_1 x_\perp^2}{2z}\right),$$

and where the correlation function $\langle a_1(\mathbf{x}_\perp, z_0) a_1^*(\mathbf{x}'_\perp, z_0) \rangle$ is given by Eq. (8). Again, in the large gain factor limit the behavior of Eq. (13) is determined by the most unstable component $\omega=0$ and in the far-field region $z \gg z_0$ one obtains

$$\langle |a_1(\mathbf{x}_\perp, z \gg z_0)|^2 \rangle \sim \exp\left\{ -\frac{x_\perp^2}{a_0^2 \tilde{z}^2} \frac{(1 + \tilde{z}_0^2)[\delta_0 + \text{Re}(\mu_0)]}{(\delta_0^2 - |\mu_0|^2)} \right\}. \quad (14)$$

From this equation one finds that the angular spreading of the backscattered beam is given by

$$\theta_1 = \theta_0 \sqrt{\frac{\delta_0^2 - |\mu_0|^2}{(1 + z_0^2/z_R^2)[\delta_0 + \text{Re}(\mu_0)]}}, \quad (15)$$

where the angle $\theta_0 = a_0/z_R \ll 1$ is the angular spreading of the incident beam. In the limit $(1/2)[\tan^{-1}(z_0/z_R)]^{-1} \ll G_R \ll (1/4)[\tan^{-1}(z_0/z_R)]^{-2}$, Eq. (15) reduces to

$$\theta_1 = \theta_0 \frac{1}{[\tan^{-1}(z_0/z_R)]^{3/2}} \sqrt{\frac{3}{4G_R}}, \quad (16)$$

in the limit $G_R \gg \max\{(1/2)[\tan^{-1}(z_0/z_R)]^{-1}, (1/4)[\tan^{-1}(z_0/z_R)]^{-2}, z_0^2/(2z_R^2)\}$ it reads

$$\theta_1 = \theta_0 G_R^{1/4} \sqrt{\frac{2}{1 + z_0^2/z_R^2}}, \quad (17)$$

and in the limit $z_0^2/(2z_R^2) \gg G_R \gg (1/2)[\tan^{-1}(z_0/z_R)]^{-1}$, it reduces to

$$\theta_1 = \theta_0 G_R^{-1/4}. \quad (18)$$

It follows from Eqs. (16)–(18) that the scattering angle θ_1 does not saturate at the same interaction length as the amplification itself. Indeed, while Eqs. (11) and (12) show that the gain factor saturates at $z_0 \sim z_R$, it can be seen from Eqs. (16)–(18) that the scattering angle saturates at a much larger interaction length $z_0 \sim z_R(2G_R)^{1/2} \gg z_R$. This important result comes from the fact that far behind the amplification region, i.e., for $z_R(2G_R)^{1/2} \gg z_0 \gg z_R$, the very low hot spot intensity can still significantly modify the phase structure of the backscattered beam (although it is negligible for what concerns the amplification). As a result, the far-field angular divergence of the backscattered beam computed at the end of the interaction region is always less than what it would be if it were computed at the end of the amplification region. For example, it is interesting to notice that although the backscattered beam is always more localized transversally than the pump beam in the amplification region, its angular spreading in the far-field zone can be *less* than the pump divergence. From Eq. (17) and the validity condition $G_R \gg 1$ one finds that this effect occurs if the inequality $z_0 > z_R(2G_R^{1/2} - 1)^{1/2} \approx z_R 2^{1/2} G_R^{1/4}$ is fulfilled (i.e., the interaction region must be long enough). Figure 1 shows the backscattering far-field

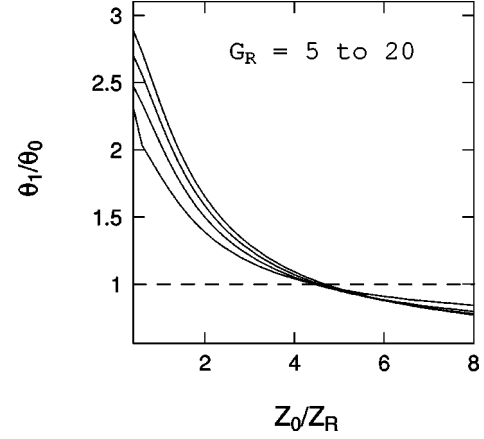


FIG. 1. Backscattering far-field angular divergence θ_1 (normalized to the angular spreading of the incident beam θ_0) as a function of the interaction half-length z_0 (normalized to the Rayleigh length z_R) for $G_R=5, 10, 15,$ and 20 , respectively, from bottom to top on the left-hand side of the figure.

angular divergence θ_1 as a function of the interaction length for different values of the gain factor G_R .

It is possible to explain this result in terms of propagation through a Gaussian aperture. Following Siegman [7], it can be seen from Eq. (6) that the plasma acts locally as a lens of radius $r_p = a_0(1 + \tilde{z}^2)/G_R^{1/2}$ and (imaginary) focal length $iz_R(r_p/a_0)^2$. When $r_p \leq r_\phi$, where $r_\phi = a_0[(1 + \tilde{z}^2)/G_R^{1/2}]^{1/2}$ is the radius of the backscattered beam [cf. Eq. (10)], one expects the coupling to modify the curvature of the backscattered light phase planes (i.e., to have an optical effect). At the end of the amplification region, $z = z_R$, one has $r_p \approx r_\phi/G_R^{1/4}$ and the plasma is still acting as a lens. At $z = z_R(4G_R)^{1/4}$, one has $r_p = r_\phi$ and $\theta_1 \approx \theta_0$. Finally, for $z \approx z_R G_R^{1/2}$, one has $r_p \gg r_\phi$ and $\theta_1 \sim \theta_0 G_R^{-1/4}$: the effect of the coupling becomes negligible. While the characteristic length for the amplification is given by z_R , the characteristic length for optical effects (i.e., phase effects) is given by $G_R^{1/2} z_R \gg z_R$.

This result is particularly important for the interpretation of the numerical simulations of backscattering instabilities from a single hot spot. The fact that the simulation box is long enough to include the amplification region is not sufficient to ensure that the far-field image of the backscattered beam does not depend on the length of the box. Our results show that for $z_0 \lesssim z_R(2G_R)^{1/2}$, it is only if the length of the simulation box is equal to the actual interaction length that numerical far-field diagnostics can be compared to experimental results straightforwardly.

V. INHOMOGENEOUS PLASMA: DESCRIPTION OF THE MODEL

We now consider the case of an inhomogeneous plasma. Within the same approximations as in Sec. II, one finds that the convective amplification of the backscattered light can be described by the system

$$\left[\partial_t + V_1 \left(\partial_z - \frac{i}{2k_1} \nabla_\perp^2 \right) \right] a_1 = \gamma_0 a_2^*, \quad (19a)$$

$$\left[\partial_t + \nu_2 \left(1 - i\varepsilon \frac{z}{z_c} \right) \right] a_2 = \gamma_0 a_1^* + S_2, \quad (19b)$$

with $\varepsilon = \text{sgn}(V_2 \kappa')$ and where $z_c = \nu_2 / |V_2 \kappa'|$ is the inhomogeneous amplification length in the strongly damped limit [8]. The inhomogeneity is taken into account in the WKB approximation by the quantity $\kappa' \equiv (d/dx)[k_0(x) - k_1(x) - k_2(x)]_{x=0}$, where $k_\alpha(x)$ is the local wave vector of wave α associated with the resonance condition that is assumed to be fulfilled at $x=0$, so that $[k_0(x) - k_1(x) - k_2(x)]_{x=0} = 0$. Laplace transforming in time system (19) and neglecting the initial condition terms, one obtains the equation for a_1

$$\left[\partial_z - \frac{i\omega}{V_1} - \frac{i}{2k_1} \nabla_\perp^2 - \frac{|\gamma_0|^2}{V_1 \nu_2 (1 - i\omega/\nu_2 + i\varepsilon z/z_c)} \right] a_1(\omega) = \frac{\gamma_0 (S_2^*)(\omega)}{V_1 \nu_2 (1 - i\omega/\nu_2 + i\varepsilon z/z_c)}. \quad (20)$$

In the following we will restrict ourselves to the cases where the plasma length $2z_0$ is smaller than the Rayleigh length z_R . It will be seen in Sec. VIII that in this limit one can neglect the longitudinal dependence of the hot spot intensity and replace Eq. (4) by

$$|\gamma_0(\mathbf{x}_\perp, z)|^2 = H(z_0^2 - z^2) \gamma^2 \exp\left[-\frac{x_\perp^2}{a_0^2}\right], \quad (21)$$

from which it follows that the longitudinal dependence of the coupling is now only due to the inhomogeneity. Expanding then the Gaussian on the left-hand side of Eq. (21) up to the first order in x_\perp^2 and defining \tilde{a}_1 by

$$a_1(\omega) = \tilde{a}_1(\omega) \exp(\vartheta),$$

with

$$\vartheta = \frac{i\omega(z-z')}{V_1} - \frac{i\varepsilon \gamma^2 z_c}{V_1 \nu_2} \ln \frac{1 + i(\varepsilon z/z_c - \omega/\nu_2)}{1 + i(\varepsilon z'/z_c - \omega/\nu_2)},$$

where z' is an arbitrary point, one finds again that the evolution (in z) of \tilde{a}_1 is given by a Schrödinger-like equation for a driven two-dimensional harmonic oscillator. Namely,

$$\left[\partial_z - \frac{i}{2k_1} \nabla_\perp^2 + \frac{\gamma^2}{V_1 \nu_2 (1 - i\omega/\nu_2 + i\varepsilon z/z_c)} \frac{x_\perp^2}{a_0^2} \right] \tilde{a}_1(\omega) = \frac{\gamma (S_2^*)(\omega) \exp(-\vartheta)}{V_1 \nu_2 (1 - i\omega/\nu_2 + i\varepsilon z/z_c)}. \quad (22)$$

VI. CONVECTIVE AMPLIFICATION BY A CYLINDRICAL INHOMOGENEOUS HOT SPOT

Following as previously the method of Ref. [6], one finds that the propagator \tilde{K}_ω of the left-hand side of Eq. (22), defined as the retarded solution to

$$\left[\partial_z - \frac{i}{2k_1} \nabla_\perp^2 + \frac{\gamma^2}{V_1 \nu_2 (1 - i\omega/\nu_2 + i\varepsilon z/z_c)} \frac{x_\perp^2}{a_0^2} \right] \times \tilde{K}_\omega(\mathbf{x}_\perp, z, \mathbf{x}'_\perp, z') = 0, \quad (23)$$

with $\lim_{z \rightarrow z'} \tilde{K}_\omega(\mathbf{x}_\perp, z, \mathbf{x}'_\perp, z') = \delta^2(\mathbf{x}_\perp - \mathbf{x}'_\perp)$, can be obtained analytically in terms of ordinary Bessel functions (cf. the appendix). Transforming back to $K_\omega = \tilde{K}_\omega \exp(\vartheta)$, one finds that the full propagator of Eq. (20) is given by

$$K_\omega(\mathbf{x}_\perp, z, \mathbf{x}'_\perp, z') = \frac{k_1 \exp[i\omega z_c (\tilde{z} - \tilde{z}')/V_1 - i\varphi + G]}{2i\pi z_c F(\tilde{z}, \tilde{z}')} \times \exp\left\{ \frac{ik_1}{2z_c} [\zeta x_\perp^2 + \zeta' x_\perp'^2 + 2\eta \mathbf{x}_\perp \cdot \mathbf{x}'_\perp] \right\}, \quad (24)$$

where $\tilde{z} = z/z_c$, $y \equiv y(\tilde{z}, \omega) = [1 + i(\varepsilon \tilde{z} - \omega/\nu_2)]^{1/2}$, $y' \equiv y(\tilde{z}', \omega)$, and with

$$\varphi = \frac{\varepsilon G_c}{2} \ln \left[\frac{1 + (\varepsilon \tilde{z} - \omega/\nu_2)^2}{1 + (\varepsilon \tilde{z}' - \omega/\nu_2)^2} \right],$$

$$G = G_c [\tan^{-1}(\tilde{z} - \varepsilon \omega/\nu_2) - \tan^{-1}(\tilde{z}' - \varepsilon \omega/\nu_2)],$$

$$\zeta = -\frac{i\varepsilon \alpha}{y} \frac{J_1(2\alpha y') Y_0(2\alpha y) - Y_1(2\alpha y') J_0(2\alpha y)}{Y_1(2\alpha y') J_1(2\alpha y) - J_1(2\alpha y') Y_1(2\alpha y)},$$

$$\zeta' = -\frac{i\varepsilon \alpha}{y'} \frac{Y_0(2\alpha y') J_1(2\alpha y) - J_0(2\alpha y') Y_1(2\alpha y)}{Y_1(2\alpha y') J_1(2\alpha y) - J_1(2\alpha y') Y_1(2\alpha y)},$$

$$\eta = -\frac{1}{F(\tilde{z}, \tilde{z}')},$$

$$F(\tilde{z}, \tilde{z}') = i\pi \varepsilon y y' [Y_1(2\alpha y') J_1(2\alpha y) - J_1(2\alpha y') Y_1(2\alpha y)],$$

where $G_c = \gamma^2 z_c / (V_1 \nu_2)$ and $\alpha = (2iG_c z_c / z_R)^{1/2}$.

The two-point correlation function at the end of the speckle is again given by Eq. (8) where the spectral density $I_\omega(\mathbf{x}_\perp, \mathbf{x}'_\perp, z_0)$ reads now

$$I_\omega(\mathbf{x}_\perp, \mathbf{x}'_\perp, z_0) = \frac{\gamma^2 z_c}{V_1^2 \nu_2^2} (2\pi)^3 \Sigma_2 \int_{x'_\perp} \int_{-\tilde{z}_0}^{\tilde{z}_0} \frac{K_\omega(\mathbf{x}_\perp, z_0, \mathbf{x}'_\perp, z'') K_\omega^*(\mathbf{x}'_\perp, z_0, \mathbf{x}_\perp, z'')}{[1 + (\tilde{z}'' - \varepsilon \omega/\nu_2)^2]} d^2 x''_\perp d\tilde{z}'', \quad (25)$$

where the propagator $K_\omega(\mathbf{x}_\perp, z_0, \mathbf{x}'_\perp, z'')$ is given by Eq. (24). As previously, in the limit of a large amplification, we can restrict ourselves to the most unstable component $\omega=0$, so that $\langle a_1(\mathbf{x}_\perp, z_0) a_1^*(\mathbf{x}'_\perp, z_0) \rangle \sim I_0(\mathbf{x}_\perp, \mathbf{x}'_\perp, z_0)$. Performing then the integrations over z'' in Eq. (25) using a steepest-descent method, one obtains

$$I_0(\mathbf{x}_\perp, \mathbf{x}'_\perp, z_0) \sim \frac{2\pi^2 \Sigma_2 k_1 \delta_0}{\nu_2 V_1 z_c} \times \exp[4G_c \tan^{-1}(\tilde{z}_0)] \times \exp\left[\frac{k_1}{2z_c}(\mu_0 x_\perp^2 + \mu_0^* x_\perp'^2 + 2\delta_0 \mathbf{x}_\perp \cdot \mathbf{x}'_\perp)\right], \quad (26)$$

with

$$\mu_0 = i\zeta_0 - \frac{\eta_0^2}{2 \operatorname{Im}(\zeta'_0)},$$

$$\delta_0 = \frac{|\eta_0|^2}{2 \operatorname{Im}(\zeta'_0)},$$

where the subscript “0” means that the quantities ζ , ζ' , and η must be evaluated at $z=z_0$, $z'=-z_0$, and $\omega=0$. The validity of Eq. (26) will be discussed in Sec. VII B.

Following the calculation of Sec. IV, one can readily obtain from Eqs. (8) and (25) the general expression of the far-field angular divergence of the backscattered light in an inhomogeneous plasma, one finds

$$\theta_1 = \theta_0 \sqrt{\left(\frac{z_R}{z_c}\right) \frac{\delta_0^2 - |\mu_0|^2}{\delta_0 + \operatorname{Re}(\mu_0)}}. \quad (27)$$

This result will be discussed in the next section where the far-field angular divergence of the backscattered beam is given in the two limits $|2\alpha y_0| \ll 1$ and $|2\alpha y_0| \gg 1$.

VII. AMPLIFICATION AND FAR-FIELD ANGULAR DIVERGENCE

A. $|2\alpha y_0| \ll 1$: No modification of the amplification due to transverse effects

In the limit $|2\alpha y_0| \ll 1$, which can be written as

$$\max(z_0, z_c) \ll \frac{z_R}{8G_c},$$

one can expand the Bessel functions in a power series of αy_0 . One then finds that the prefactor δ_0 on the right-hand side of Eq. (26) does not yield any exponential contribution to the amplification. It follows that there is no diffraction effect on the usual one-dimensional convective gain $G_{conv} = 4G_c \tan^{-1}(z_0/z_c)$ in this limit. For what concerns the angular divergence in the far-field zone, one obtains the two following asymptotic results: (i) in the limit $z_R/(2G_c) \ll z_0 \ll z_c$ one recovers the homogeneous result of Eq. (16),

$$\theta_1 = \theta_0 \frac{1}{(z_0/z_R)^{3/2}} \sqrt{\frac{3}{4G_c}},$$

and in the opposite limit $z_0 \gg z_c$ one finds

$$\theta_1 = \theta_0 \frac{1}{(z_0/z_R)^{1/2}} \frac{(z_R/z_c)}{\sqrt{4G_c}}. \quad (28)$$

These results will be compared to those of the simpler cylindrical model, where any longitudinal dependence of the coupling is neglected, in Sec. VIII.

B. $|2\alpha y_0| \gg 1$: Reduction of the amplification due to transverse effects

In the opposite limit

$$\max(z_0, z_c) \gg \frac{z_R}{8G_c},$$

one can replace the Bessel functions by the leading term of their asymptotic expansion. A careful study of integral (25) shows that the most important contribution comes from the vicinity of $z=-z_0$ for $\varepsilon=-1$, and from the vicinity of $z=\max[-z_0, -z_c(G_R/2)^{1/3}]$ for $\varepsilon=+1$. Accordingly, in the case $\varepsilon=+1$, the validity of Eq. (26) is limited to the domain

$$z_0 < z_c \left(\frac{G_R}{2}\right)^{1/3}. \quad (29)$$

The last condition that remains to be checked is that the radius of the backscattered beam is smaller than that of the pump beam in order for the parabolic approximation of $\exp(-r^2/a_0^2)$ to be valid. From Eqs. (25) and (24), one finds that the region of the sources that contribute significantly to the backscattered beam is located at the entrance of the interaction region and has a radius of $(z_c/k_1)^{1/2} |\operatorname{Im}(\zeta'_0)|^{-1/2}$. On the other hand, from Eq. (26) one finds that the radius of the backscattered beam at the end of the interaction region is given by $(z_c/k_1)^{1/2} |\operatorname{Re}(\mu_0)|^{-1/2} \approx (z_c/k_1)^{1/2} |\operatorname{Im}(\zeta_0)|^{-1/2}$. Demanding that these radius be smaller than a_0 and using the relation $z_R = k_1 a_0^2$, one obtains the condition

$$\frac{z_R}{z_c} \min(|\operatorname{Im}(\zeta'_0)|, |\operatorname{Im}(\zeta_0)|) > 1.$$

This inequality ceases to be satisfied either at the front side [$|\operatorname{Im}(\zeta'_0)| < |\operatorname{Im}(\zeta_0)|$], or at the back side [$|\operatorname{Im}(\zeta'_0)| > |\operatorname{Im}(\zeta_0)|$] of the hot spot, depending on the sign of ε . In both cases it reads

$$\left(\frac{2G_c z_R}{z_0}\right)^{1/2} \sin\left[\frac{\pi}{4} - \frac{1}{2} \tan^{-1}\left(\frac{z_0}{z_c}\right)\right] = \left(\frac{G_R z_c}{z_0}\right)^{1/2} \left[1 - \left(\frac{z_0^2}{z_c^2 + z_0^2}\right)^{1/2}\right]^{1/2} > 1,$$

which reduces to Eq. (29) in the limit $z_0 \gg z_c$. We therefore conclude that in both cases $\varepsilon = \pm 1$ and in the limit $z_0 \gg z_c$, the validity of Eq. (26) reduces to Eq. (29).

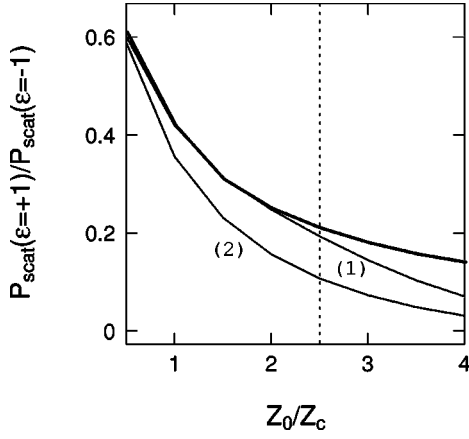


FIG. 2. Dissymmetry of the backscattered power as a function of the interaction half-length z_0 (normalized to the amplification length z_c), depending on the sign of the gradient in an inhomogeneous plasma. The thick line corresponds to the analytical result Eq. (31). Curves (1) and (2) correspond to numerical solutions to Eqs. (22) and (20) (keeping the Gaussian coupling) respectively, with $G_c=20$ and $z_R/z_c=5$. The vertical dashed line shows the limit of validity (29) of Eq. (26) as explained in the text.

Unlike the first case VII A, there is now a diffraction effect on the usual one-dimensional convective gain due to the fact that the prefactor δ_0 on the right-hand side of Eq. (26) yields an exponential contribution to the amplification. In the validity domain (29), one finds that the convective gain factor for the backscattered power is given by

$$G_{conv} = 4G_c \tan^{-1}\left(\frac{z_0}{z_c}\right) - 4\left(\frac{2G_c z_c}{z_R}\right)^{1/2} \left[\left(1 + \frac{z_0^2}{z_c^2}\right)^{1/2} - 1 \right]^{1/2}. \quad (30)$$

It is worth noticing that expression (30) is the same for $\varepsilon = \pm 1$. On the other hand, since the local radius of the backscattered beam $(z_c/k_1)^{1/2} |\text{Re}(\mu_0)|^{-1/2}$ does depend on the sign of ε , one is led to the remarkable result that the backscattered power P_{scat} depends also on the sign of ε . One finds, namely,

$$\frac{P_{scat}(\varepsilon = +1)}{P_{scat}(\varepsilon = -1)} = \left[1 + 2\frac{z_0^2}{z_c^2} + 2\frac{z_0}{z_c} \left(1 + \frac{z_0}{z_c}\right)^{1/2} \right]^{-1/2}, \quad (31)$$

which reduces to $z_c/(2^{1/2}z_0) \ll 1$ in the limit $z_0 \gg z_c$. We have compared these analytical results to numerical solutions of Eq. (22) and Eq. (20) [i.e., without expanding the Gaussian in Eq. (21)] in which the instability grows from a constant boundary condition at $z = -z_0$ (cf. Fig. 2). It can be seen that the dissymmetry of the backscattered power is slightly more pronounced when one keeps the Gaussian coupling [curve (2)] as compared to our analytical prediction. This is due to the fact that the $\varepsilon = -1$ backscattered beam is wider than the $\varepsilon = +1$ one after the maximum amplification region (see the discussion at the end of this section), which leads to a slight underestimation of $P_{scat}(\varepsilon = -1)$ when one replaces the Gaussian coupling by its quadratic approximation.

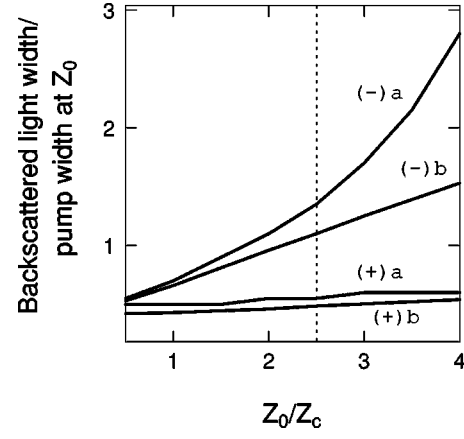


FIG. 3. Backscattered beamwidth at the end of the interaction region in an inhomogeneous plasma as a function of the interaction half-length z_0 (normalized to the amplification length z_c). Curves labeled $(\varepsilon)b$ correspond to the analytical results of Sec. VI depending on the sign of ε . Curves labeled $(\varepsilon)a$ correspond to numerical solutions to Eq. (20) (keeping the Gaussian coupling), the parameters are the same as in Fig. 2.

The angular divergence of the backscattered beam in the far-field zone depends also on the sign of ε . In the limit $z_c \ll z_0 < z_c(G_R/2)^{1/3}$, one finds

$$\theta_1 = \theta_0 \sqrt{2} G_R^{1/4} \left(\frac{2z_0}{z_c}\right)^{\varepsilon/4}. \quad (32)$$

This dependence on the sign of the inhomogeneity gradient can be explained in terms of propagation of the backscattered light through a Gaussian duct [7]. Locally the plasma can be regarded both as a Gaussian aperture acting like a lens of imaginary focal length $iz_c(1+\tilde{z}^2)/G_c$ and an ordinary lens of focal length $f = \varepsilon z_c(1+\tilde{z}^2)/(\tilde{z}G_c)$. If $\varepsilon = -1$, the plasma acts as a converging lens ($f > 0$) before the maximum amplification region ($|z/z_c| < 1$), and as a diverging lens ($f < 0$) after the maximum amplification region (conversely if $\varepsilon = +1$). The backscattered light produced before the maximum amplification region is therefore more concentrated on the axis when it reaches this region, which increases the reflectivity in this case. Since the situation is opposite for $\varepsilon = +1$, the reflectivity is greater for $\varepsilon = -1$ than for $\varepsilon = +1$. After the maximum amplification region, the diverging effect ($f < 0$) widens the backscattered beam in the $\varepsilon = -1$ case. The radius of the backscattered beam at the end of the interaction region ($z = z_0$) is thus less for $\varepsilon = +1$ than for $\varepsilon = -1$, and, due to diffraction, the far-field divergence at $z \gg z_0$ is greater for $\varepsilon = +1$ than for $\varepsilon = -1$. Figure 3 shows the backscattered beam width at the end of the interaction region as a function of the interaction length.

VIII. COMPARISON WITH THE CYLINDRICAL MODEL

It is interesting to compare the previous results with the ones obtained in the case of a ‘‘cylindrical’’ hot spot of length L for which Eq. (4) is replaced by

$$|\gamma_0(\mathbf{x}_\perp, z)|^2 = H(L^2/4 - z^2) \gamma^2 \exp\left[-\frac{x_\perp^2}{a_0^2}\right]. \quad (33)$$

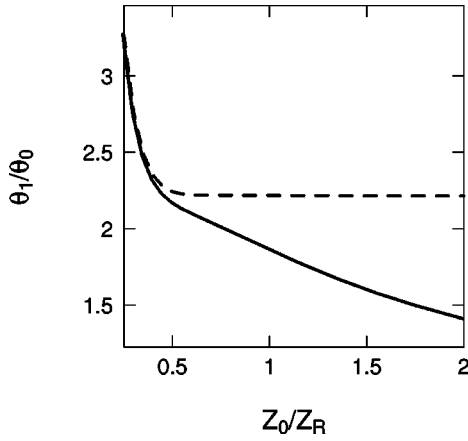


FIG. 4. Backscattering far-field angular divergence θ_1 (normalized to the angular spreading of the incident beam θ_0) as a function of the interaction half-length z_0 (normalized to the Rayleigh length z_R) for $G_R=5$. The solid line corresponds to Eq. (15) in which the z dependence of the hot spot intensity is kept. The dashed line corresponds to the ‘‘cylindrical model’’ result of Refs. [4] and [5].

The latter expression corresponds to the simple model considered by Eliseev *et al.* [4] and Tikhonchuk, Mounaix, and Pesme [5]. In this case the convective gain G_{conv} is given by Eqs. (11) and (12) in which $2 \tan^{-1}(z_0/z_R)$ is replaced by $\tilde{L} \equiv L/z_R$, and the ratio θ_1/θ_0 is given by Eq. (15) in which one sets $z_0=0$ and redefines the quantities α and ϕ_0 as $\alpha = (2iG_R)^{1/2}$ and $\phi_0 = \alpha\tilde{L}$. In the limit $1/(2\tilde{L}) \ll G_R \ll 1/(2\tilde{L}^2)$ one obtains

$$G_{conv} = 2G_R\tilde{L}, \quad (34)$$

$$\theta_1 = \theta_0 \frac{1}{\tilde{L}^{3/2}} \sqrt{\frac{6}{G_R}}, \quad (35)$$

and in the opposite limit $G_R \gg \max[1/(2\tilde{L}), 1/(2\tilde{L}^2)]$, one has

$$G_{conv} \approx 2G_R\tilde{L} \left(1 - \frac{1}{\sqrt{G_R}} \right), \quad (36)$$

$$\theta_1 = \theta_0 2^{1/2} G_R^{1/4}, \quad (37)$$

[i.e., one recovers the angular spreading (17) with $z_0^2 \ll z_R^2$]. These results are in agreement with those of Refs. [4] and [5] obtained in the limit of a small interaction region $L \ll z_R$.

In the case of a homogeneous plasma, it can be seen from Eqs. (34),(36), and Eqs. (11),(12) that one can easily obtain the proper value of the convective gain of a Gaussian hot spot by considering an ‘‘effective’’ cylindrical hot spot of length $L = L_{eff} \equiv 2z_R \tan^{-1}(z_0/z_R)$. On the other hand, it follows from Eqs. (35),(37) and Eqs. (16)–(18) that the far-field angular divergence of the backscattered light from this effective cylindrical hot spot always overestimates the actual angular spreading. In the case of a cylindrical hot spot, θ_1 saturates at $\theta_1 = \theta_0 2^{1/2} G_R^{1/4} > \theta_0$ (cf. Fig. 4), while in the case of a Gaussian hot spot it saturates at $\theta_1 = \theta_0 G_R^{-1/4}$, which is less than θ_0 , for $z_0 \gg z_R (2G_R)^{1/2}$. It is only if $z_0 \lesssim z_R$ that one can properly estimate the far-field angular divergence of the

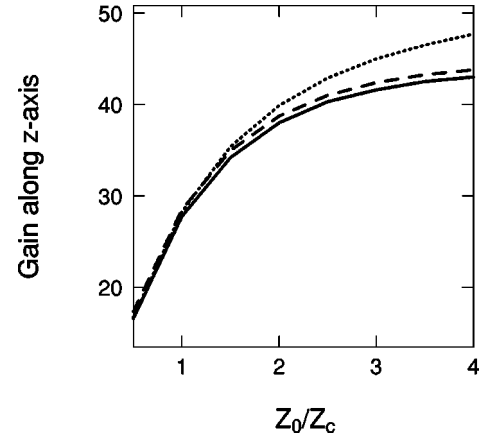


FIG. 5. Hot spot convective gain in the case of an inhomogeneous plasma as a function of the interaction half-length z_0 (normalized to the amplification length z_c). The solid line shows the analytical result (30) in which the z dependence of the coupling is kept. The dotted line is the cylindrical model result of Ref. [5]. The dashed line corresponds to a numerical solution to Eq. (20) (with Gaussian coupling); the parameters are the same as in Fig. 2.

backscattered light from a Gaussian hot spot by considering an effective cylindrical hot spot of the same gain.

In the case of an inhomogeneous plasma, one cannot recover the exact value of the convective gain from an effective cylindrical hot spot of length $L = L_{eff} \equiv 2z_c \tan^{-1}(z_0/z_c)$. Comparing Eq. (30) and the convective gain given by the cylindrical model, one finds that the latter gives a good approximation of Eq. (30) only if

$$\frac{2^{1/2}(\sqrt{1+z_0^2/z_c^2}-1)^{1/2}}{\tan^{-1}(z_0/z_c)} \simeq 1,$$

which is fulfilled as long as $z_0/z_c \leq 2.5$ (cf. Fig. 5). It follows, in particular, that the cylindrical approximation breaks down in the limit of strongly inhomogeneous plasmas where one has $z_0/z_c \gg 1$. For what concerns the far-field angular divergence of the backscattered light, one has, in the strongly inhomogeneous plasma limit $z_0/z_c \gg 1$,

$$\frac{\theta_1}{\theta_{1cyl}} = \frac{\pi^{3/2}}{24^{1/2}} \frac{1}{(z_0/z_c)^{1/2}} \simeq \frac{1.14}{(z_0/z_c)^{1/2}} \ll 1 \quad (38)$$

in the case $|2\alpha y_0| \ll 1$, where there is no diffraction effect on the amplification (cf. Sec. VII A), which corresponds to case I of Ref. [5], and

$$\frac{\theta_{1\pm}}{\theta_{1cyl}} = \left(\frac{2z_0}{z_c} \right)^{\pm 1/4} \quad (39)$$

in the opposite limit $|2\alpha y_0| \gg 1$ where diffraction effects reduce the amplification (cf. Sec. VII B), which corresponds to case II of Ref. [5]. In these equations θ_1 and $\theta_{1\pm}$ are, respectively, given by Eqs. (28) and (32), and θ_{1cyl} denotes the angular spreading obtained from the cylindrical model of Ref. [5]. It can be seen that, in the strongly inhomogeneous plasma limit $z_0/z_c \gg 1$, the cylindrical approximation does not yield the proper far-field angular divergence of the backscattered light (cf. Fig. 6).

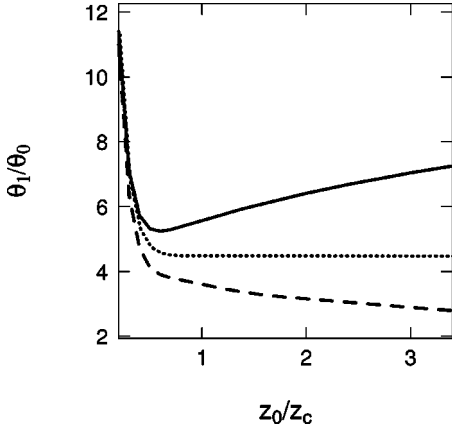


FIG. 6. Backscattering far-field angular divergence θ_1 (normalized to the angular spreading of the incident beam θ_0) in an inhomogeneous plasma, as a function of the interaction half-length z_0 (normalized to the amplification length z_c). The solid and dashed lines corresponds to the analytical result (27) for $\varepsilon = +1$ and $\varepsilon = -1$, respectively. The dotted line is the cylindrical model result of Ref. [5]. The parameters are the same as in Fig. 2.

IX. CONCLUSION

In this paper we have studied the problem of backscattering instabilities from a single laser hot spot in the frame of the paraxial approximation. We have performed an exact analytical calculation of the convective gain factor and of the far-field angular divergence of the backscattered light in the two cases of homogeneous and inhomogeneous plasmas.

In the case of homogeneous plasmas, where the longitudinal dependence of the coupling reduces to that of the hot spot intensity, we have obtained expressions for the convective gain factor that generalize those of Eliseev *et al.* [4] to the case of an arbitrary value of the interaction length. We have shown that the far-field angular divergence is determined not only by the amplification *within* the hot spot but also by the propagation of the backscattered light *behind* the amplification region, where the hot spot intensity is negligible for what concerns the amplification. We have found that the far-field angular divergence of the backscattered light computed at the end of the interaction region is always less than what it would be if it was computed at the end of the amplification region. For a long enough interaction region, namely, for $z_0/z_R > 2^{1/2} G_R^{1/4}$ with $G_R \gg 1$, it is even found to be *less* than the pump divergence.

In the case of inhomogeneous plasmas, where the longitudinal dependence of the coupling is only due to the inhomogeneity, we have obtained expressions for the convective gain factor and for the far field angular divergence of the backscattered light. In the limit of practical interest $\max(z_0, z_c) \gg z_R (8G_c)^{-1}$, with $z_0 < z_c (G_R/2)^{1/3}$, $G_c \gg 1$, and $G_R \gg 1$, we have found that both the power and the far-field angular divergence of the backscattered beam depend on the sign of the inhomogeneity gradient. This remarkable result follows from focusing or defocusing optical effects occurring *outside* the resonance region, where the coupling is negligible for what concerns the amplification.

It is worth mentioning that all these results should be taken into account in the interpretations of numerical and/or experimental far-field images of the backscattered beam in

terms of its near-field structure.

We have then compared our results to previous ones obtained in the case of a cylindrical hot spot. For homogeneous plasmas, we have found that the far-field angular divergence of the backscattered light can be properly estimated by considering an effective cylindrical hot spot of the same gain in the limit $z_0 \lesssim z_R$ only. For inhomogeneous plasmas, we have found that the cylindrical model always overestimates the on-axis linear convective gain factor, and that this model breaks down in the limit $z_0 \gg z_c$ where the plasma is strongly inhomogeneous.

ACKNOWLEDGMENTS

The authors would like to thank D. Pesme, V. T. Tikhonchuk, and T. W. Johnston for many fruitful discussions they had with them on this topic.

APPENDIX: DERIVATION OF THE GREEN'S FUNCTIONS

In this appendix we show how to calculate the propagators (7) and (24). The problem reduces to find the Green's function $G(\mathbf{x}_\perp, z, \mathbf{x}'_\perp, z')$ defined as the retarded solution to

$$\left[\partial_z - \frac{i}{2k_1} \nabla_\perp^2 + \frac{1}{l_G} \frac{x_\perp^2}{a_0^2} q(z)^2 \right] G(\mathbf{x}_\perp, z, \mathbf{x}'_\perp, z') = 0, \quad (\text{A1})$$

with $\lim_{z \rightarrow z'} G(\mathbf{x}_\perp, z, \mathbf{x}'_\perp, z') = \delta^2(\mathbf{x}_\perp - \mathbf{x}'_\perp)$. Following the method of Ref. [6], one has

$$G(\mathbf{x}_\perp, z, \mathbf{x}'_\perp, z') = \frac{k_1}{2i\pi f} \exp \left[\frac{ik_1}{2f} (\dot{f} x_\perp^2 - 2\mathbf{x}_\perp \cdot \mathbf{x}'_\perp + g x_\perp'^2) \right], \quad (\text{A2})$$

where dot means z derivative and the functions f and g are solutions to

$$\dot{f} = \frac{2i}{l_G z_R} q(z)^2 f,$$

$$f(z') = 0,$$

$$\dot{f}(z') = 1,$$

and

$$\ddot{g} = \frac{2i}{l_G z_R} q(z)^2 g,$$

$$g(z') = 1,$$

$$\dot{g}(z') = 0,$$

with $z_R \equiv k_1 a_0^2$.

1. Gaussian hot spot in a homogeneous plasma

In the case of a Gaussian hot spot in a homogeneous plasma considered in Sec. III, one has $q(z) = [1$

$+(z/z_R)^2]^{-1}$ and $l_G = V_1(\nu_2 - i\omega)/\gamma^2$. It is then useful to write f and g as $\exp\int^z k(z')dz'$, which yields a Riccati equation for k ,

$$\dot{k} + k^2 = \frac{2i}{l_G z_R} q(z)^2.$$

Inserting the expression of $q(z)$ into this equation and trying $k(z) = (a + bz)/[1 + (z/z_R)^2]$, one obtains the equation

$$\left(a^2 + b - \frac{2i}{l_G z_R}\right) + 2a\left(b - \frac{1}{z_R^2}\right)z + b\left(b - \frac{1}{z_R^2}\right)z^2 = 0,$$

the solution to which reads

$$a = \pm \alpha/z_R,$$

$$b = 1/z_R^2,$$

with $\alpha \equiv (2iz_R/l_G - 1)^{1/2}$. One has, therefore,

$$k(z) = \frac{1}{z_R} \frac{z/z_R}{1 + (z/z_R)^2} \pm \frac{\alpha}{z_R} \frac{1}{1 + (z/z_R)^2},$$

and from the boundary conditions for f and g , one obtains straightforwardly

$$f = (z_R/\alpha) \sqrt{1 + (z/z_R)^2} \sqrt{1 + (z'/z_R)^2} \sinh(\phi), \quad (\text{A3a})$$

$$\dot{f} = \frac{\sqrt{1 + (z'/z_R)^2}}{\sqrt{1 + (z/z_R)^2}} \left[\cosh(\phi) + \frac{z}{\alpha z_R} \sinh(\phi) \right], \quad (\text{A3b})$$

$$g = \frac{\sqrt{1 + (z/z_R)^2}}{\sqrt{1 + (z'/z_R)^2}} \left[\cosh(\phi) - \frac{z'}{\alpha z_R} \sinh(\phi) \right], \quad (\text{A3c})$$

where $\phi \equiv \alpha[\tan^{-1}(z/z_R) - \tan^{-1}(z'/z_R)]$. Inserting Eqs. (A3) into Eq. (A2) gives the solution to Eq. (6), which yields the full propagator (7).

2. Cylindrical hot spot in a inhomogeneous plasma

In the case of a cylindrical hot spot in a inhomogeneous plasma considered in Sec. VI, one has $q(z) = [1 + i(\varepsilon z/z_c - \omega/\nu_2)]^{-1/2}$, $l_G = V_1 \nu_2/\gamma^2$, and the equation for f and g reads

$$\left[1 + i\left(\varepsilon \frac{z}{z_c} - \frac{\omega}{\nu_2}\right)\right] \ddot{h} - \frac{2i}{l_G z_R} h = 0, \quad (\text{A4})$$

where h denotes f or g . This equation can be solved explicitly in terms of ordinary Bessel functions. Defining $y = q(z)$, $y' = q(z')$, and taking into account the boundary conditions for f and g , one obtains

$$f = iz_c \pi \varepsilon y y' [Y_1(2\alpha y') J_1(2\alpha y) - J_1(2\alpha y') Y_1(2\alpha y)], \quad (\text{A5a})$$

$$\dot{f} = \alpha \pi y' [Y_0(2\alpha y) J_1(2\alpha y') - J_0(2\alpha y) Y_1(2\alpha y')], \quad (\text{A5b})$$

$$g = \alpha \pi y [Y_0(2\alpha y') J_1(2\alpha y) - J_0(2\alpha y') Y_1(2\alpha y)], \quad (\text{A5c})$$

where $\alpha = (2iG_c z_c/z_R)^{1/2}$. Inserting Eqs. (A5) into Eq. (A2) gives the solution to Eq. (23), which yields the full propagator (24).

- [1] H. A. Rose and D. F. DuBois, Phys. Rev. Lett. **72**, 2883 (1994).
 [2] H. A. Rose and D. F. DuBois, Phys. Fluids B **5**, 590 (1993); J. Adler, *The Geometry of Random Fields* (Wiley, New York, 1981).
 [3] M. R. Amin *et al.*, Phys. Fluids B **5**, 3748 (1993); V. V. Eliseev *et al.*, Phys. Plasmas **2**, 1712 (1995).
 [4] V. V. Eliseev, W. Rozmus, V. T. Tikhonchuk, and C. E. Capjack, Phys. Plasmas **3**, 3754 (1996).

- [5] V. T. Tikhonchuk, Ph. Mounaix, and D. Pesme, Phys. Plasmas **4**, 2658 (1997).
 [6] *Selected Problems in Quantum Mechanics*, edited by D. Ter Haar (Infosearch, London, 1964), p. 147.
 [7] A. Siegman, *Lasers* (University Science Books, Mill Valley, 1986), p. 786.
 [8] D. Pesme, G. Laval, and R. Pellat, Phys. Rev. Lett. **31**, 203 (1973).